3D Study on the Effect of Process Parameters on the Cooling of Polymer by Injection Molding

Hamdy Hassan,[1] Nicolas Regnier,[1] Cyril Pujos,[2] Guy Defaye[1]

[1]*Laboratoire TREFLE-Bordeaux1-UMR 8508, Site ENSCPB, 16 avenue Pey Berland, Pessac Cedex 33607, France*
[2]*ISMANS, 44 avenue Bartholdi, Le Mans 72000, France*

Received 14 April 2009; accepted 26 May 2009
DOI 10.1002/app.30812
Published online 16 July 2009 in Wiley InterScience (www.interscience.wiley.com).

ABSTRACT: Plastic injection molding (PIM) is well known as a manufacturing process to produce products with various shapes and complex geometry at low cost. Determining optimal settings of process parameters critically influence productivity, quality, and cost of production in the PIM industry. To study the effect of the process parameters on the cooling of the polymer during injection molding, a full three-dimensional time-dependent injection molding analysis was carried out. The studied configuration consists of a mold having cuboids-shaped cavity with two different thicknesses and six cooling channels. A numerical model by finite volume was used for the solution of the physical model. A validation of the numerical model was presented. The effect of different process parameters (inlet coolant temperature, inlet coolant flow rate, injection temperature, and filling time) on the cooling process was considered. The results indicate that the filling time has a great effect on the solidification of the product during the filling stage. They also show that low coolant flow rate increases the heterogeneity of the temperature distribution through the product. The process parameter realizing minimum cooling time not necessary achieves optimum product quality and the complete filling of the cavity by the polymer material. © 2009 Wiley Periodicals, Inc. J Appl Polym Sci 114: 2901–2914, 2009

Key words: process parameter; injection molding; polymer; solidification; cooling

INTRODUCTION

The manufacturing industry for plastic products has been growing rapidly in recent years, and more and more plastics are used widely to substitute for metals.[1] The injection molding process is one of the most widely used processing methods for manufacturing plastic products. It is characterized by high degree of automation, high productivity, and good dimensional stability of moldings.[2] Injection molding is a cyclic process of forming plastic into a desired shape by forcing the molten polymeric resin under pressure into an evacuated cavity.[3] The injection molding cycles starts by filling the mold cavity with hot polymer melt at injection temperature which is called "filling stage." After the cavity filling stage, additional molten polymer is packed into the cavity at a higher pressure to compensate the expected shrinkage as the polymer solidifies "postfilling stage." This is followed by "cooling stage," where the mold is cooled until the part is sufficiently rigid to be ejected. The last step is the "ejection stage" in which the mold is opened and the part is ejected.[4] Several factors are involved in the injection molding process and have a great effect on the final quality of plastic products. These factors can be classified into four categories: materials, molding machine, model design, and process conditions.[5] In the cooling system design of injection molding, the geometric parameters (radius and location of each cooling channels) and process parameters (i.e., inlet coolant temperature, volumetric flow rate of cooling fluid, filling time, injection temperature, etc.) should be considered.[6] Determining optimal settings of process parameter critically influence productivity, quality, and cost of production in the plastic injection molding (PIM) industry. Previously, production engineers used either trial-and-error method or Taguchi's parameter design method to determine optimal settings of process parameter for PIM.[7] However, these methods are unsuitable in present PIM because of the increasing complexity of product design and the requirement of multiresponse quality characteristics. The effect of process parameters on different product properties and injection molding performance has aroused the interest of various researchers. Malguarnera and Manisali[8] studied the effect of process parameters on the tensile properties of weld lines in injection molded thermoplastics. They found that increasing the mold temperature increases the yield strength of both the weld and nonweld samples. For semicrystalline polymers, the yield stress is mostly affected by the mold temperature. The strain at yield appears to be insensitive to the processing conditions examined. For amorphous polymers displaying a

Correspondence to: H. Hassan (hamdyaboali@yahoo.com).

yield, elongation at break is the property most affected by the processing conditions. Bushko and Stokes[9,10] studied the effect of process conditions on the shrinkage, warpage, and residual stresses of thermo viscoelastic melt between two parallel plates. Their results showed that a higher packing pressure resulted in a lower shrinkage, both in the in-plane and through-thickness directions. Higher mold temperature increased shrinkage in the through-thickness direction, but it had no effect for the shrinkage of the in-plane direction. Lau et al.[11] presented the application of artificial neural networks in suggesting the change of molding parameters for improving dimensional quality (length) of injection molded parts based on the concept of reverse process modeling. Therefore, product weight and product length are feasible quality characteristics that can be used as important responses in the process parameter optimization of PIM. Wu and Liang[12] used six process parameters (mold temperature, packing pressure, melt temperature, injection velocity, injection acceleration, and packing time) to discuss the effects of process parameters on the weld-line width of injection molded plastic products. Chiang and Chang[13] used four control process parameters (mold temperature, melt temperature, injection pressure, and injection time) to determine the optimal settings of initial process parameter for injection molded plastic parts with a thin shell feature and under multiple quality characteristic considerations. Ghosh et al.[14] studied the effect of process parameters on the mechanical properties of product by injection molding. The results show that the maximum shear stress and maximum shear rate are mainly controlled by melt processing temperature and injection flow rate, respectively. With an increase in injection flow rate, the shear stress and increment of bulk temperature were increased more at low melt processing temperature compared with high melt processing temperature. Yu et al.[6] considered the geometric parameters (radius and location of cooling channel) and the process parameters (volumetric flow rate of cooling fluid, inlet cooling temperature, packing time, and cooling time) in the cooling system design of injection molding. In their study, a mold cooling system for 15 inches display was optimized by combined Kriging model and computer-aided engineering model. The results indicate that the quality of the product parts can be improved by optimization of the operating parameters

In this article, a three-dimensional study is presented for the effect of the process parameters on the solidification and temperature of polystyrene material by injection molding. The polymer material has the form of cuboids with two different thicknesses. The polymer material is cooled by water that flows through six cooling channels as shown in Figure 1. A finite volume model is used for the solution of the physical governing equations. A validation of the numerical model with an analytical solution is presented. Different process parameters (inlet coolant temperature, inlet coolant flow rate, injection temperature, and filling time) are considered. Their effect on the time required to completely solidifying the polymer and the percentage of the solidified polymer during the filling stage is studied.

MATHEMATICAL MODEL

The mathematical equations governing the physical model must take into considerations: the injection of the polystyrene material into the mold cavity, the solidification of the polymer material during the cooling process, and the flow of the cooling fluid inside the cooling channels.

During the filling, cooling, solidification, and ejection of the product, the following assumptions are introduced for the mathematical model.

The polystyrene material and the cooling water flowing inside the cooling channels are considered noncompressible fluids.

The physical and thermal properties (ρ, λ, C_P) of the polystyrene, mold, and cooling water are considered constant during the numerical simulation.

Generally, the mathematical equations governing the physical model are the mass, momentum, and energy equations:

$$\nabla.V = 0 \tag{1}$$

$$\rho\left[\frac{\partial V}{\partial t} + (V\nabla).V\right] = -\nabla P + \rho g + \nabla.(\tau) \tag{2}$$

$$\rho C_P\left[\frac{\partial T}{\partial t} + (V\nabla).T\right] = \nabla(\lambda\nabla T) + \eta\dot{\gamma}^2 \tag{3}$$

In addition to the conservation laws, the polymer viscosity is function of shear rate, temperature, and pressure. The rheological behavior of the polymer material is described by a Cross type equation[15]:

$$\eta = \frac{\eta_0(T,p)}{1 + \left[\eta_0(T,p)\frac{\dot{\gamma}}{\tau^*}\right]^{1-n}} \tag{4}$$

where τ^* is a critical stress level.

The zero shear rate viscosity η_0 is presented by[15]:

$$\eta_0(T,p) = B\exp\left(\frac{T_b}{T}\right)\exp(\beta p) \tag{5}$$

The rheological model constants of the selected polystyrene material are listed in Table I.[16]

The momentum equation is closely coupled with the viscosity constitutive relation. The following simple linear averages are adopted to approximate the

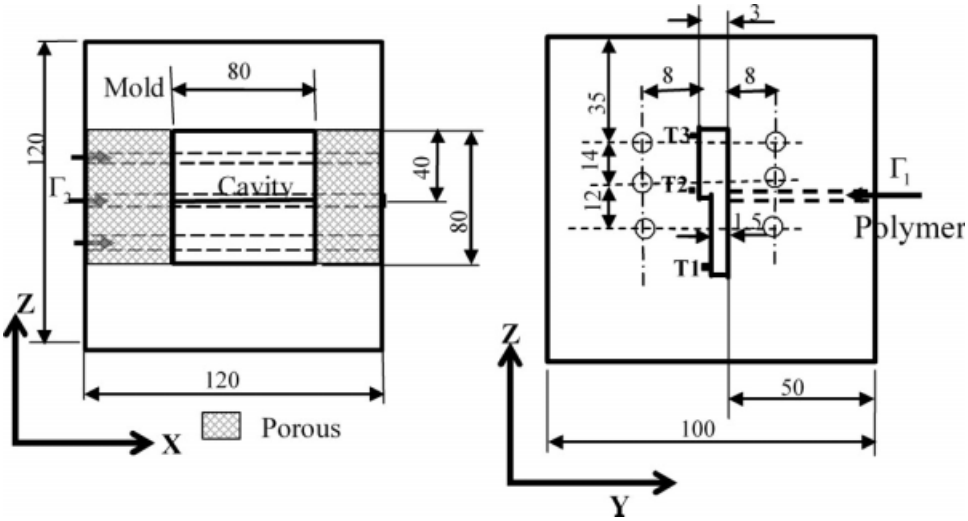

Figure 1 Configuration of the mold, mold cavity, and cooling channels (dimensions mm).

viscosity and density at the interface between the polymer melt inlet to the mold cavity and the air inside the cavity[17]:

$$\begin{cases} \rho = \rho_a + \left(\rho_p - \rho_a\right)C \\ \mu = \mu_a + \left(\mu_p - \mu_a\right)C \end{cases} \quad (6)$$

The fractional volume function C is defined as follows:

$$C = \begin{cases} 1 \text{ for the point inside polymer} \\ 0 \text{ for the point inside air} \end{cases} \quad (7)$$

Then, the interface is located within the cells where $0 < C < 1$. The volume fraction function is governed by a transport equation:

$$\frac{\partial C}{\partial t} + V.\nabla C = 0 \quad (8)$$

This equation determines the movement of interface position between the polymer and the air.

To take into account the solidification, a source term is added to the energy equation corresponding to heat absorption or heat release,[18] which takes in consideration the absorption or the dissipation of the heat through phase change process. This technique is validated in previous studies.[18,19] The energy eq. (3) in this case is represented as follows:

$$\rho C_P \left[\frac{\partial T}{\partial t} + (V\nabla).T\right] = \nabla.(\lambda\nabla T) + \eta\dot{\gamma}^2 + S_c \quad (9)$$

The source term S_c is represented by:

$$S_c = \rho L \frac{\partial f_s}{\partial t} \quad (10)$$

where $f_s(T) = 0$ at $T > T_f$ (fully liquid region), $0 < f_s < 1$ at $T = T_f$ (isothermal phase change region), and $f_s(T) = 1$ at $T < T_f$ (fully solid region).

The following boundary conditions are used.

At the inlet of the mold cavity:

During filling stage, constant inlet flow rate and isothermal conditions are assumed for the polymer as shown in Figure 1:

$$Q = Q_p \quad \text{and} \quad T = T_p \quad \text{on } \Gamma_1 \quad (11)$$

During cooling stage, zero inlet velocity and adiabatic condition for the temperature are assumed at Γ_1.

At the inlet of the cooling channels:

$$Q = Q_c \quad \text{and} \quad T = T_c \quad \text{on } \Gamma_2 \quad (12)$$

At mold side walls, adiabatic boundary conditions are assumed.

TABLE I
The Rheological Model Constants

Material constant	Value
n	2.7×10^{-01}
τ^* (Pa)	2.31×10^{04}
B (Pa s)	3.04×10^{-9}
T_b (K)	133 000
β (Pa^{-1})	3.5×10^{-8}

NUMERICAL SOLUTION

The numerical solution of the mathematical model governing the behavior of the physical system is computed by finite volume method. The equations are solved by an implicit treatment for the different terms of the equations system. The discretized equations are solved by an iterative algorithm of

Augmented Lagrangien. In our numerical solution, we use the concept of a unique system of equations which is solved in the whole numerical domain (one fluid model). Penalization terms are added to the general system of equations,[20] to take into account different boundary conditions and solid mold zone. Using this technique of unique system makes the numerical discretization simpler to program and matches with various physical model.

Solid obstacles

To deal with solid mold within the numerical domain, it is possible to use multigrid domains, but it is often very much simpler to implement the Brinkman theory.[20] The numerical domain is then considered as a unique porous medium. The permeability coefficient K defines the capability of a porous medium to let pass the fluids more or less freely through it. If this permeability coefficient is great ($K \rightarrow +\infty$), the medium is equivalent to a fluid. If the permeability coefficient is small ($K \rightarrow 0$), then the medium is equivalent to a solid. A real porous medium is modeled with intermediate values of K. With this technique, it is also possible to model moving rigid boundaries or complex geometries.

To take this coefficient K into account in our system of equations, an extra term, called Darcy term $\frac{\mu}{K}V$[20] is added to the momentum eq. (2), and then the momentum equation becomes:

$$\rho\left[\frac{\partial V}{\partial t} + (V\nabla)_V\right] = -\nabla P + \rho g + \nabla.(\tau) - \frac{\mu}{K}V \qquad (13)$$

Practically, values of $K = 10^{+20}$ (liquid) and $K = 10^{-20}$ (solid) are imposed to obtain these conditions.

Boundary conditions

To deal with the boundary conditions within the numerical domain, the method consists of writing a generalized boundary condition as a surface flux[21]:

$$-\left(\frac{\partial V}{\partial N}\right)_{\text{surface}} = B_V(V - V_\infty) \qquad (14)$$

where B_V is a matrix. It has to be noted that it is a vectorial formulation and then involves the three Cartesian components of the velocity vector V. The boundary condition is directly taken into account in eq. (13) then, we have the following equation

$$\rho\left[\frac{\partial V}{\partial t} + (V\nabla).V\right] + B_V(V - V_\infty) = -\nabla P + \rho g + \nabla.(\tau) - \frac{\mu}{K}V \qquad (15)$$

Thanks to this penalization term, we can then impose a velocity in the numerical domain or on a lateral boundary. For $B_V = 0$, Neumann boundary conditions are modeled where $\left(\frac{\partial V}{\partial N}\right) = 0$. Some coefficients are chosen as $B_V = +\infty$ to ensure Dirichlet boundary conditions imposed at the mesh grid points of the boundary. This formulation enables to easily modify the boundary conditions while passing from the condition of Neumann to a condition of Dirichlet.

The same procedure is used to impose the boundary condition in case of the Energy equation. The quantity $B_T(T - T_\infty)$ is introduced in eq. (9) and then the following equation for the energy is solved:

$$\rho C_P\left[\frac{\partial T}{\partial t} + (V\nabla).T\right] + B_T(T - T_\infty) = \nabla.(\lambda\nabla T) + \eta\dot{\gamma}^2 + S_c \qquad (16)$$

where

$$B_T = 0 : \text{Neumann condition}\left(\frac{\partial T}{\partial n} = 0\right) \qquad (17)$$

$$B_T \rightarrow \infty : \text{Dirichlet condition}(T = T_\infty) \qquad (18)$$

Further details on the numerical model are available in Refs. 22 and 23. To validate this numerical model, an analytical solution known in the case of the filling of a square cavity is used.

Validation

Filling a square cavity:

The example consists of filling a unit square cavity where a velocity field is imposed at the boundary as shown in Figure 2, where:

$$u = -y \qquad (19)$$

$$V = -x$$

Since the velocity is steady, the particle pathlines and the streamlines are coincident, and governed by[24]:

$$y^2 = x^2 + C_1 \qquad (20)$$

where, C_1 is a constant.

The magnitude of the velocity vector $|U|$ is equal to $(x^2 + y^2)^{1/2}$. The initial front is assumed as straight lines (ab) and (bc). As the fluid fills the square cavity from the top and right sides, the velocity diminishes and vanishes at the origin o. Since the particle at the point b will flow along the square diagonal. Then, the analytical solution of the nondisplacement (r/R) versus filling time (t) is[24]:

$$r/R = 1 - e^{-t} \qquad (21)$$

where r is the particle displacement $|oo^*|$ and R is the length of the diagonal $|bo|$ as shown in Figure 2.

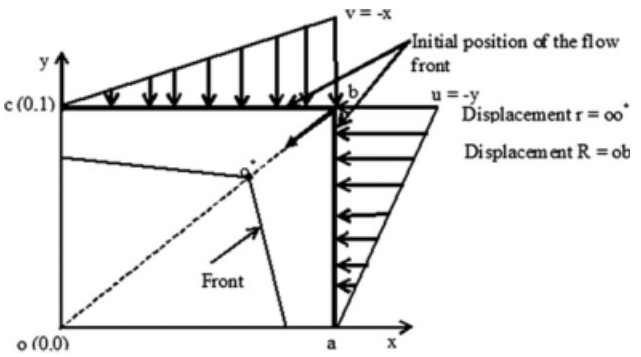

Figure 2 Flow front through a filling of square cavity within a given velocity field.

To compare the numerical solution with the analytical solution, the flow front position at the diagonal is calculated at various times. A good agreement between the numerical solution and the analytical solution is obtained during the entire filling process where the number of grids 127×127 as shown in Figure 3. Figure 4 represents the mesh grid study at instant of filling time equals to 3 s. It shows that the spatial convergence is obtained with two order convergence, where the error percent is obtained by the following equation:

$$\text{Error percent} = \frac{\left|(r/R)_{num} - (r/R)_{th}\right|}{(r/R)_{th}} \qquad (22)$$

The figure shows that when the number of grids decrease, the error increases and the maximum error is about 4% at number of grids of (40×40). Another methods of validation of this model is available in Ref. 25.

RESULTS AND DISCUSSION

A full three-dimensional time-dependent injection molding analysis is carried out for a mold with cuboids-cavity of two different thicknesses as shown in Figure 1. The cooling of the product is carried out by using cooling water flowing through six cooling channels. All the cooling channels have the same size and they are 8 mm diameter. The cooling operating parameters and the material properties used in this study are listed in Tables II and III, respectively.[16,26] They are considered as a reference case and constant during all numerical simulation except the cases illustrated within the text.

In our numerical model, each numerical simulation consists of three main stages: filling stage at which hot polymer is injected to the mold cavity at constant temperature and constant flow rate, cooling stage where the polymer injected is cooled until the end of cooling time and the ejection stage, where the

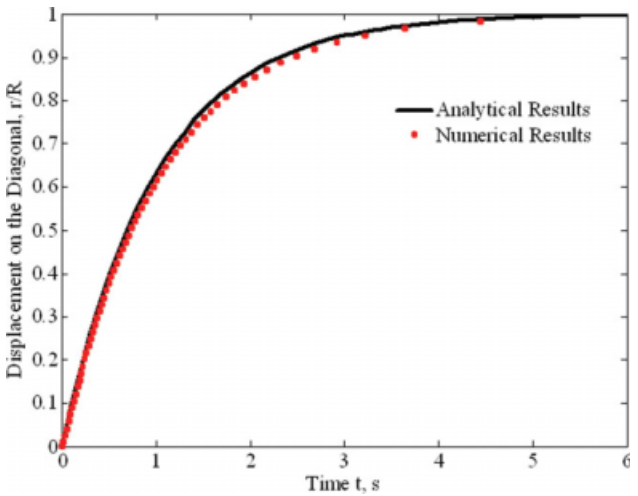

Figure 3 Comparison of the numerical results with the analytical solution at number of grids 127×127. [Color figure can be viewed in the online issue, which is available at www.interscience.wiley.com.]

cavity is assumed filled with air which is initially at ambient temperature.

The mold cavity must be completely filled with hot polymer, so it is assumed that the air is escaping from the mold cavity through a thinned layer of porous media having the same properties of mold material with thickness of 1 mm as shown in Figure 1. According to eq. (15), the permeability factor K determines the capability of a porous media to let the fluid pass more or less freely through it. According to the Darcy law[27]

$$V = -\frac{K}{\mu}\nabla P \qquad (23)$$

By considering the air viscosity, the injection pressure, the time required to withdraw the air from the cavity (filling time), and the total volume of the

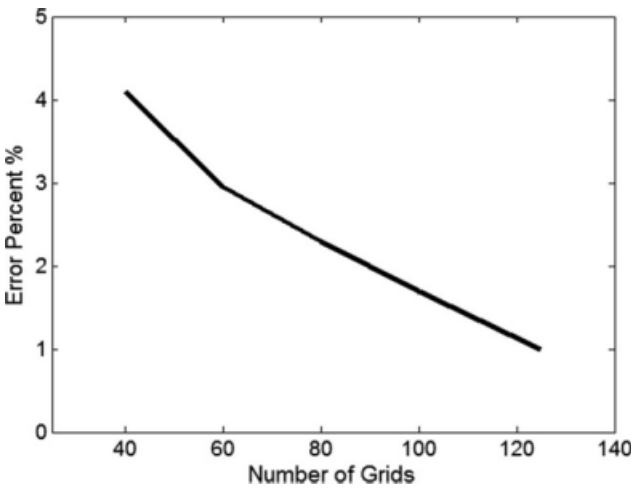

Figure 4 Change of the error percent with the number of grids at instant of time equals 3 s.

TABLE II
Cooling Process Parameters (Reference Case)

Cooling operating parameter	Value	Cooling operating parameter	Value
Inlet temperature of the coolant fluid	30°C	Time of filling stage	4.2 s
Injected temperature of polymer	220°C	Time of cooling stage	39.5 s
Melting temperature of polymer	110°C	Mold opening time	3 s
Latent heat	115 kJ kg^{-1} K^{-1}	Diameter of the cooling channels	8 mm
Temperature of ambient air	30°C	Flow rate of cooling water	$8.5e^{-5}$ m^3 s^{-1}

mold cavity, it is found that the value of permeability K must not be less than 10^{-12} m^2. Figure 5 shows the effect of the permeability factor K of the porous medium on the percentage of filled cavity volume and the inlet pressure to the cavity. It shows that when the permeability factor increases, the filled volume of the cavity with polymer material decreases. It also shows that when the value of K increases, the inlet pressure decreases. When the value of K increases, the polymer material would escape to the porous medium and because of the flow rate of the polymer to the cavity is constant, then the filled volume of the cavity with polymer decreases. The K value of 1×10^{-10} m^2 is chosen because it gives the maximum percentage of the cavity volume filled with polymer. It is also adequate for the air to escape from the mold cavity and to trap the polymer inside the cavity during the filling process. Moreover, it provides at the inlet to the cavity a pressure equivalent to the pressure of the injection molding machine (25–75 MPa).[16]

The mold temperature is an important factor in injection molding thermoplastics and has a significant influence on the injection molding cycle and the quality of molded parts. The cavity temperature influences the surface quality, after-shrinkage, orientation, residual stresses, and the morphology of semicrystalline polymers. The lower the cavity temperature, the higher the orientation, residual stresses, and density of the amorphous border layer of semicrystalline plastic products and the lower the surface quality.[28] Figure 6 shows the cyclic transient variations of the mold temperature with time for the first 25 cycles for locations T1, T2, and T3 (Fig. 1) at the mold wall. It is found that the simulated results are in good agreement with the transient characteristic of the cyclic mold temperature variations described in Refs. 26 and 29. The figure shows that the relative temperature fluctuation is larger near the inlet position to the mold cavity (T2) and diminishes away from that position (T1 and T3). We find that the maximum amplitude of temperature fluctuation during the steady cycle can reach 20°C and the minimum fluctuation is about 7°C. The result shows that the cyclic mold temperature (the variation of the mold temperature at each cycle) reaches to steady state after about 20 cycles.

TABLE III
Material Properties

Material	Density (kg m^{-3})	Specific heat (J kg^{-1} K^{-1})	Conductivity (W m^{-1} K^{-1})
Mold	7,670	426	36.5
Polymer	938	2,280	0.18
Cooling water	1,000	4,185	0.6
Air	1.17	1,006	0.0263

An efficient cooling system of injection molding aims at reducing cycle time and reduces operation cost. It must also minimize such undesired defects like sink marks, differential shrinkage, built-up thermal residual stress, and product warpage and achieves uniform temperature distribution through the product.[29] To study the effect of different process parameters on the performance of injection molding process, different process parameters are taken in to consideration during the simulation and their values are shown in Table IV. During this study, all the operation parameters are taken constant according to the reference case except the values of the studied process parameter.

Effect of cooling fluid

The heat of the molten polymer is taken away by the coolant moving through the cooling channels and by the air around the exterior mold surface. It is found that 95% of the heat of the molten polymer

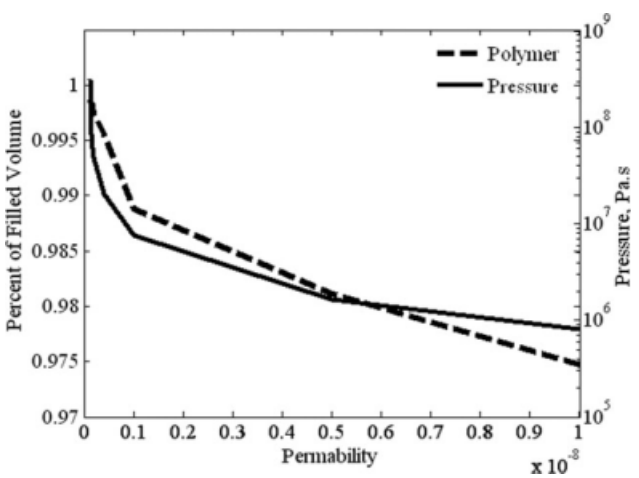

Figure 5 Changing the percent of volume filled—and inlet pressure to the cavity—with changing of permeability factor K.

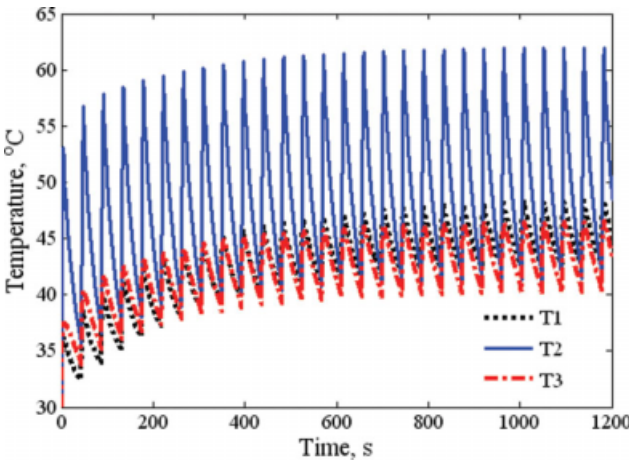

Figure 6 Temperature history of the first 25 cycles for locations T1 to T3 at mold wall. [Color figure can be viewed in the online issue, which is available at www.interscience.wiley.com.]

must be removed by the coolant which is passing through the cooling channels.[29] The cooling fluid flowing through the cooling channels must be able to remove the heat at the required rate so that the plastic part can be ejected completely solidified without any distortion.

Effect of cooling fluid temperature

Decreasing time spent on cooling the product before it is ejected would drastically increase the production rate, and hence would reduce costs. Figure 7 shows the effect of inlet temperature of the cooling fluid on the time required for completely solidifying the product at different injection molding cycles. Figure 7 indicates that the time required to completely solidifying the product decreases by decreasing the inlet fluid temperature. It also shows that the cooling time increases with increasing injection molding cycles due to heating of the mold material. The figure shows that the cooling time reaches to steady state (constant value) after about 20 cycles and at low inlet fluid temperature the cooling time increases slightly with increasing injection molding cycles. From the results, it is found that a decrease of coolant temperature by about 35% will decrease the cooling time by about 10%.

TABLE IV
Values of the Studied Process Parameters

Process parameter	Values range
Cooling fluid temperature, T_c (°C)	21–33
Flow rate of cooling fluid, Q (m^3/s)	3×10^{-6} to 1.4×10^{-4}
Injection polymer temperature, T_P (°C)	200–240
Filling time, t_{fill} (s)	3.2–5.7

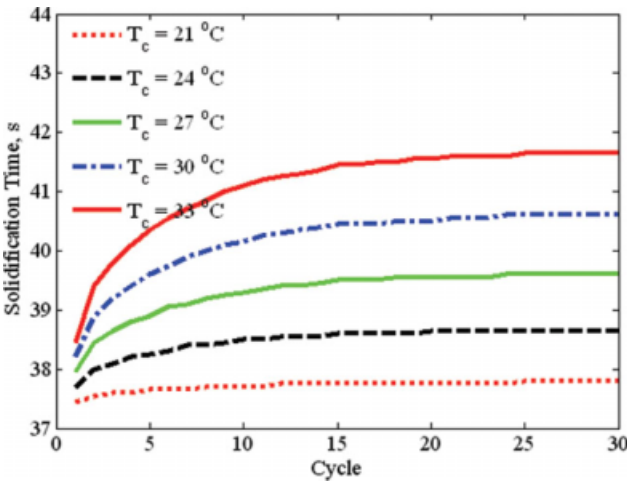

Figure 7 The variation of the solidification time with increasing injection molding cycles at different cooling fluid temperature. [Color figure can be viewed in the online issue, which is available at www.interscience.wiley.com.]

During the filling process and due to low mold temperature, a skin layer solidifies instantaneously beside the mold walls. Increasing this skin layer during the filling stage leads to increase the pressure required to fill the mold cavity. It also has a negative effect on the product quality. Because of the compelling flow under a low temperature and higher shear rate, a large molecular orientation is created and frozen in the skin layer.[30] Then, it is recommended to avoid the solidification of the product during the filling stage. The effect of the inlet temperature of the coolant fluid on the solidification percent of the product at the end of filling stage for different cooling cycles is shown in Figure 8. Solidification percent represents the ratio of the mass of product solidified

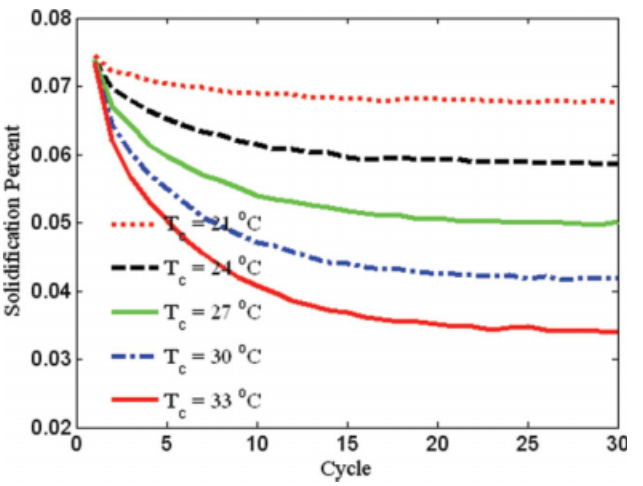

Figure 8 Variation of the solidification percent at the end of filling stage with increasing injection molding cycles at different temperature of cooling fluid. [Color figure can be viewed in the online issue, which is available at www.interscience.wiley.com.]

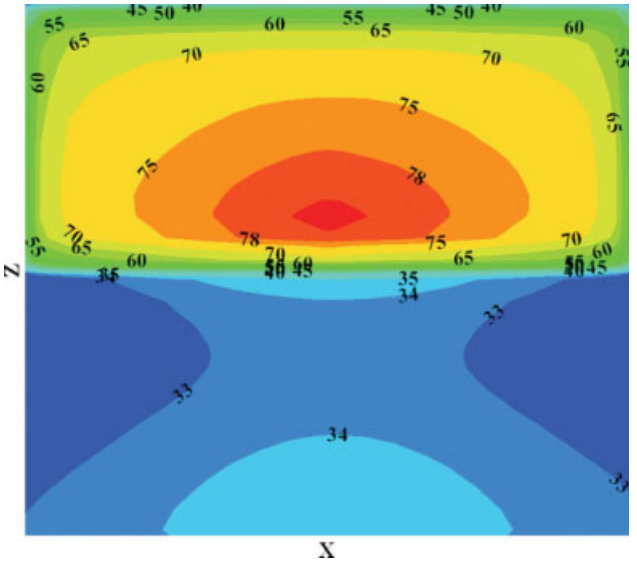

Figure 9 Temperature distribution through the product at the end of cooling stage for *XZ* plane for 30th injection molding cycle at $T_c = 21°C$ ($Y = 0.0485$). [Color figure can be viewed in the online issue, which is available at www .interscience.wiley.com.]

to the total mass of the product, i.e., the volume of the product solidified to the total volume of the product. The figure shows that the solidification percent increases with decreasing the inlet temperature of the cooling fluid. It also indicates that at low inlet coolant temperature, solidification of the polymer is almost constant with the increasing injection molding cycles. Thus, signifies that the mold temperature does not increase significantly with increasing mold

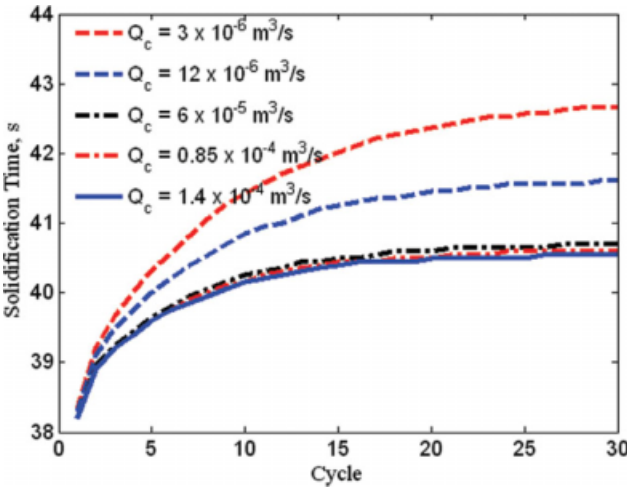

Figure 11 Variation of the solidification time with increasing injection molding cycles at different coolant flow rate. [Color figure can be viewed in the online issue, which is available at www.interscience.wiley.com.]

cycle contrarily in case of high cooling fluid temperature.

Study of the temperature distribution in molded parts is of fundamental importance to more complete understanding of many complicated phenomena such as heat transfer problems and molecular orientation, etc, which in turn can lead to the improved design of processing equipment and control for molded products of specified dimensions. The measurement of the temperature distribution during the molding processes is also of great importance for the validation of numerical simulation

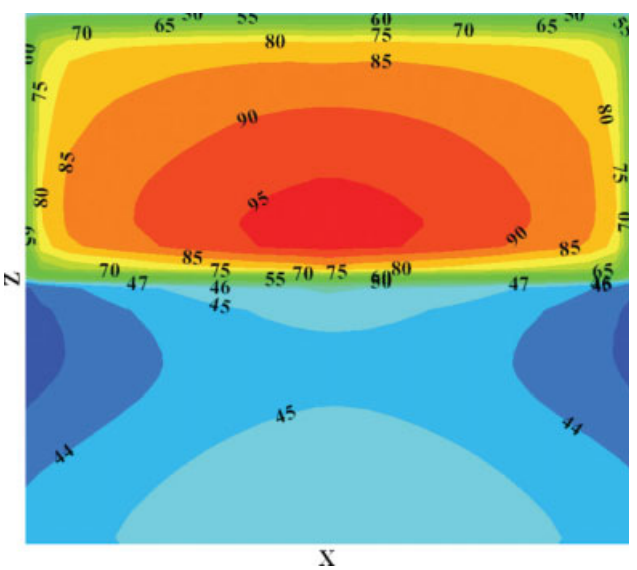

Figure 10 Temperature distribution for *XZ* plane through the product at the end of cooling stage for 30th injection molding cycle at $T_c = 33°C$ ($Y = 0.0485$). [Color figure can be viewed in the online issue, which is available at www. interscience.wiley.com.]

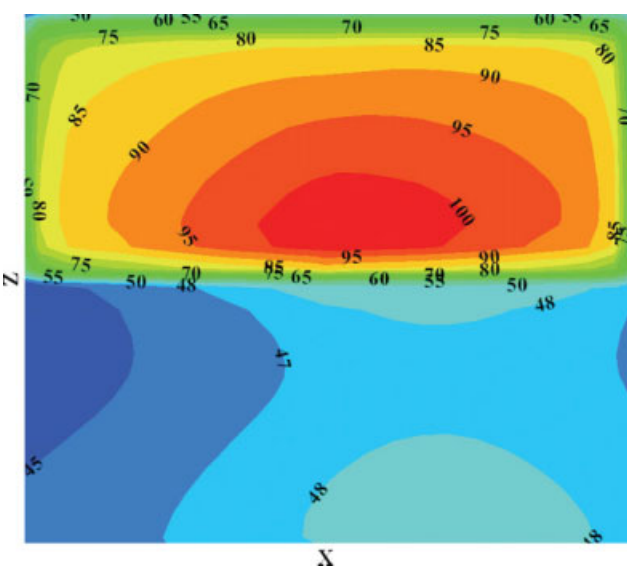

Figure 12 Temperature distribution for section *XZ* through the product at the end of cooling stage for 30th injection molding cycle at $Q_c = 3\times10^{-6}$ m^3/s ($Y = 0.0485$ m). [Color figure can be viewed in the online issue, which is available at www.interscience.wiley.com.]

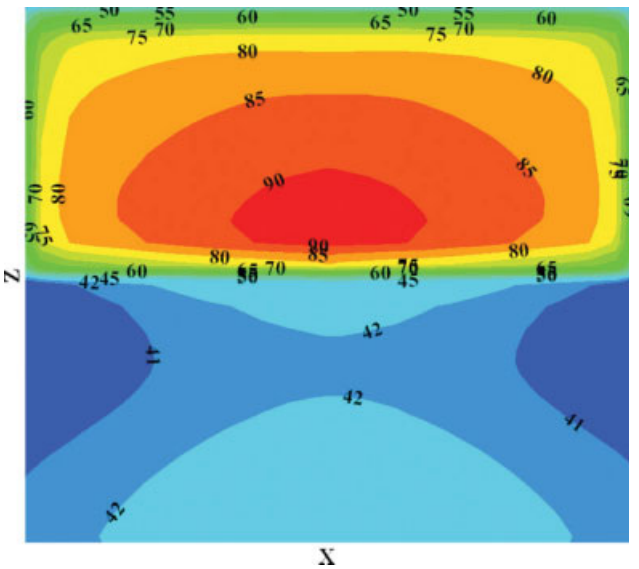

Figure 13 Temperature distribution for section *XZ* through the product at the end of cooling stage for 30th injection molding cycle at $Q_c = 1.4\times10^{-4}$ m^3/s ($Y = 0.0485$ m). [Color figure can be viewed in the online issue, which is available at www.interscience.wiley.com.]

models.[31] The temperature distribution at the end of cooling stage for *XZ* plane of the product at coolant temperature 21°C and 33°C are shown in Figures 9 and 10, respectively. The temperature distributions through the thin part show that the surface region of the polymer has lower temperature due to rapid heat transfer to the cold mold walls. Contrarily, the temperature of the core region of the thick part is higher because it is not readily affected by the heat transfer to mold and the low thermal diffusivity of polymer material. The figures show that the maximum difference of the temperature between the thick and thin part is about the same for the two cases and they also have the same profile of temperature distribution. From the values of the temperatures of the product, it is found that a decreasing of the coolant temperature will increase the cooling rate of the product during the cooling stage which affects the final product quality.

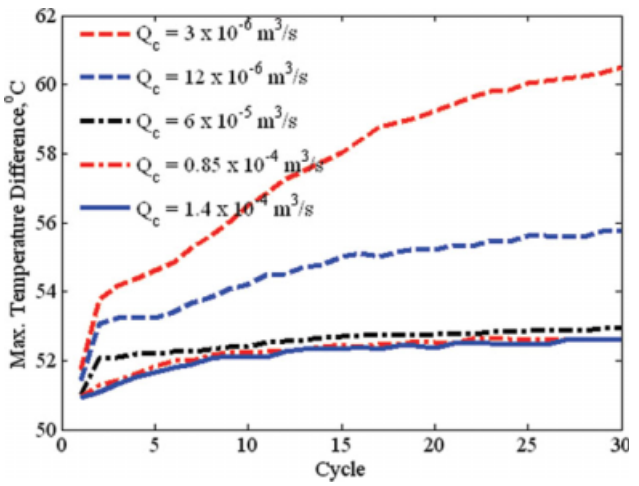

Figure 14 Evolution of the maximum difference of the temperature through the product at the end of cooling stage for different coolant flow rate with increasing injection molding cycles. [Color figure can be viewed in the online issue, which is available at www.interscience.wiley.com.]

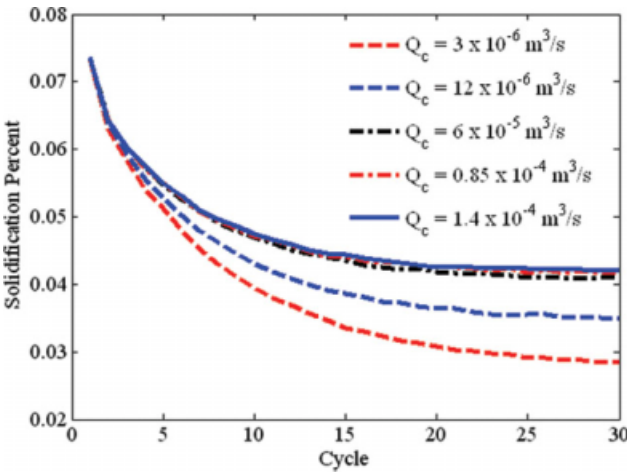

Figure 15 Evolution of the solidification percent at the end of filling stage for different coolant flow rates with increasing injection molding cycles. [Color figure can be viewed in the online issue, which is available at www.interscience.wiley.com.]

Effect of flow rate of cooling fluid

The amount of the heat removed from the polymer material depends on the flow rate and the inlet temperature of the cooling fluid flowing through the cooling channels. Increasing coolant flow rate requires increasing pump capacity required to pump

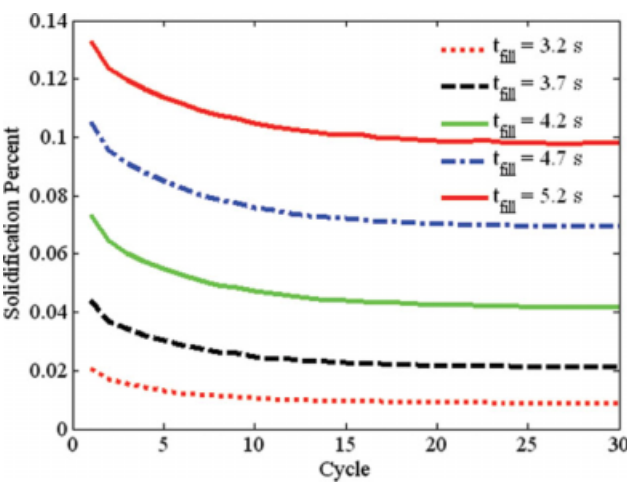

Figure 16 Evolution of the solidification percent at the end of filling stage for different filling times with increasing injection molding cycles. [Color figure can be viewed in the online issue, which is available at www.interscience.wiley.com.]

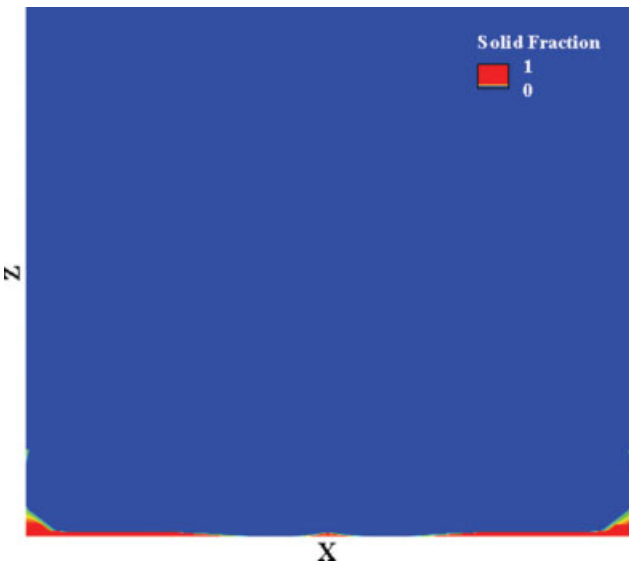

Figure 17 Solidification distribution for plane *XZ* of polymer material at the end of filling stage for 30th injection molding cycle and at $t_{fill} = 3.2$ s ($Y = 0.0485$ m). [Color figure can be viewed in the online issue, which is available at www.interscience.wiley.com.]

the fluid through the cooling channels and hence increases the process cost. The effect of the coolant flow rate on the time required for completely solidifying the product at different injection molding cycles is shown in Figure 11. The figure shows that the solidification time increases with decreasing the coolant flow rate and this effect increases with increasing injection molding cycles. The figure also shows that at higher cooling flow rate, the solidification time has almost the same value and is not affected by the value of the cooling flow rate. The great value of the coolant flow rate helps the mold temperature to reach a steady state faster. Figure 11 shows that at higher cooling flow rate, the solidification time reaches approximately to constant value after about 15 injection molding cycles. The optimal value of the coolant flow rate is about 6×10^{-5} and greater than this value, the increase of the coolant flow rate does not have any effect on the solidification process

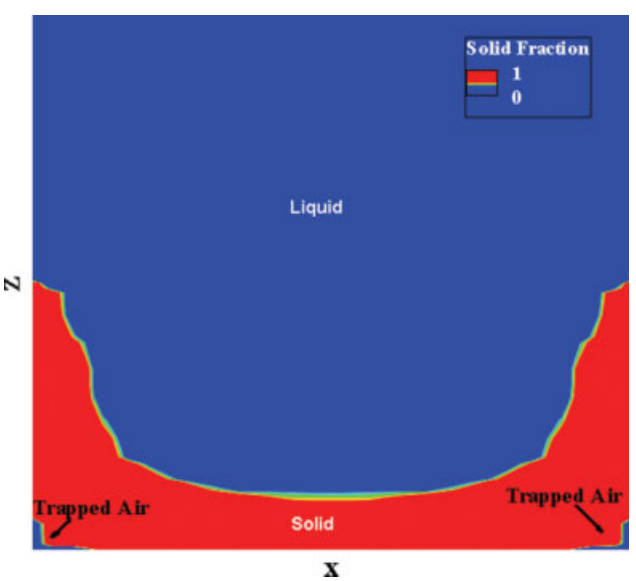

Figure 18 Solidification distribution at plane *XZ* of polymer material at the end of filling stage for 30th injection molding cycle and at $t_{fill} = 5.7$ s ($Y = 0.0485$ m). [Color figure can be viewed in the online issue, which is available at www.interscience.wiley.com.]

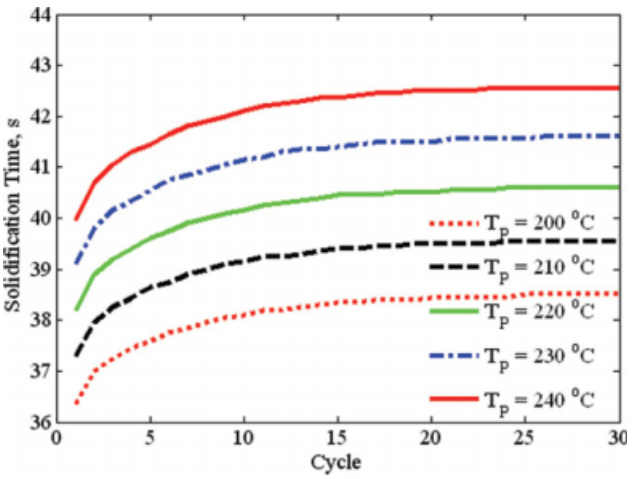

Figure 19 Evolution of the solidification time with increasing injection molding cycles at different polymer temperature. [Color figure can be viewed in the online issue, which is available at www.interscience.wiley.com.]

Thermal conductivity of plastic is slower than that of metals, therefore, differences of the cooling velocity part by part due to partial temperature gradient is appeared during the cooling of plastic material. Those differences produce different molding shrinkage and internal residual stresses, which cause warps and cracks in the plastic molded products in some years after the molding. If the plastic materials in the solidification process are controlled well and cooled down uniformly, it is expected that the generation of the residual stress can be reduced much.[32] Therefore, the coolant fluid, which reduces the cooling time, must perform uniform temperature distribution through the product. The effect of coolant flow rates 3×10^{-6} and 1.4×10^{-4} on the temperature distribution through the cross section of the product *XY* is shown in Figures 12 and 13, respectively. The results are shown for the 30th cycles of the injection molding. The figures show that in case of low coolant flow rate, the temperature increases with increasing *X* direction more than the case of higher coolant flow rate. It signifies that the coolant flow rate is not sufficient to extract the heat of the product along *X* direction, which affects the homogeneity of the temperature distribution through the product. From the temperature distribution, it is found that the

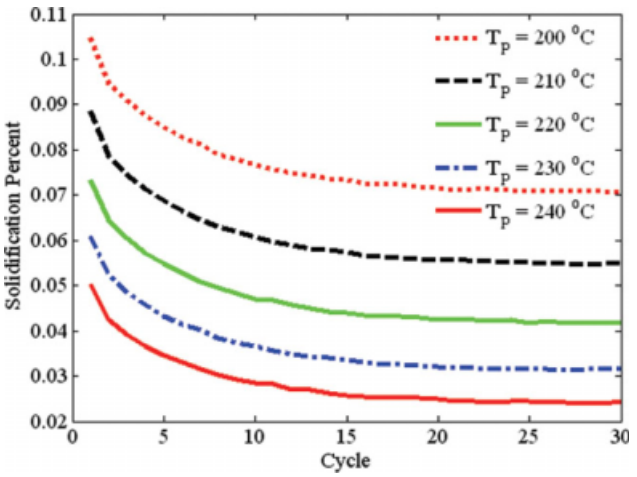

Figure 20 Evolution of the solidification percent at the end of filling stage with increasing injection molding cycles at different polymer temperature. [Color figure can be viewed in the online issue, which is available at www.interscience.wiley.com.]

maximum temperature of the product is always beneath the filling position (Fig. 1). Figures 12 and 13 show that the area located near the cooling channel experienced more cooling which leads to further decreasing in temperature and the region away from the cooling channel experienced less cooling effect. Thus, it leads to a separation in the temperature distribution through the thin part which affects the final product quality. The figures also show that the temperature of thick part is greater than the temperature of thin part and the difference in the temperature between the thin and thick part is greater in case of low coolant flow rate. Those results are clear when we compare the maximum difference of temperature through the product at the end of cooling stage for different coolant flow rates as shown in Figure 14. Figure 14 shows that the maximum difference of temperature through the product in case of lower coolant flow rate is higher and increases with increasing injection molding cycles. It also shows that, in case of higher coolant flow rate, the maximum difference of the temperature through the product is not affected by the value of the coolant flow rate.

As indicated, the solidification layer during the filling stage must be minimized or eliminated as possible. The effect of coolant flow rate on the solidification percent of the polymer at the end of filling stage is shown in Figure 15. Figure 15 shows that the solidification percent decreases with increasing molding cycles. It also shows that at higher values of coolant flow rate, the increase in the coolant flow rate has not effect on the solidification percent.

Effect of filling time

Filling the mold cavity as rapidly as possible should keep the polymer melt at high temperatures for a filling time. When the filling time increases (slower flow rates), the viscous resistance decreases, resulting in a lower filling pressure. For very short filling times, very high pressure is required to drive the melt into the mold cavity as it is practiced for thin wall molding where melt pressures of 200 MPa are commonly used.[33] In this case, the polymer flow is dominated by high internal heat generation, significant heat convection with the moving polymer melt, and relatively low heat loss by conduction to the mold.[33] It is also desirable to operate at the minimum pressure from an energy conservation viewpoint, but there may be a trade off with an increase in cycle time.[34] The effect of filling time on the solidification percent of the polymer at the end of filling stage for different injection molding cycles is shown in Figure 16. The figure shows that the filling time has a great effect on the solidification of the product during the filling process. It also shows that the solidification percent of the product increases with

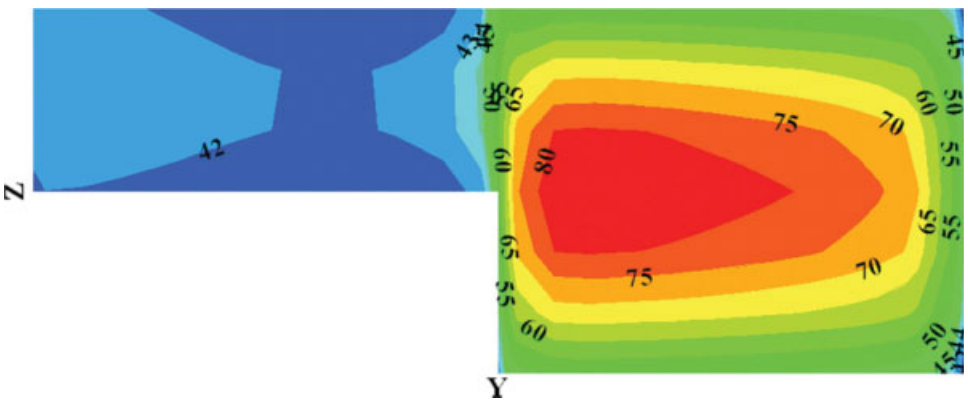

Figure 21 Temperature distribution for section *YZ* through the product at the end of cooling stage for 30th injection molding cycle at TP = 200°C (X = 0.06 m). [Color figure can be viewed in the online issue, which is available at www.interscience.wiley.com.]

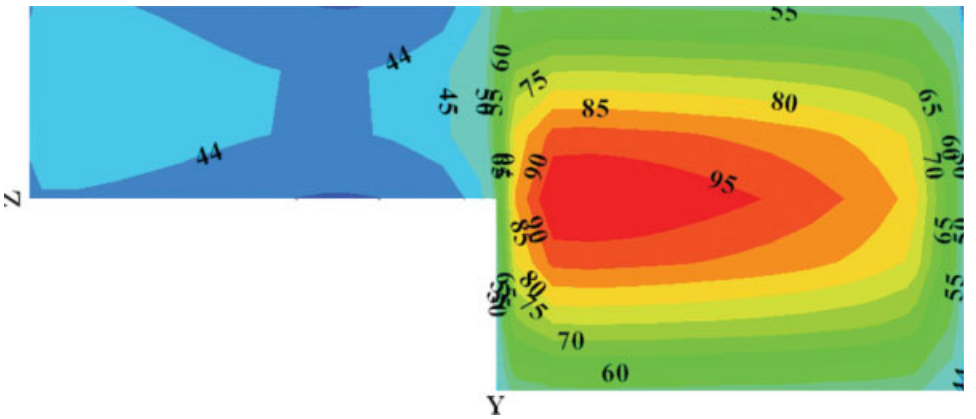

Figure 22 Temperature distribution for section *YZ* through the product at the end of cooling stage for 30th injection molding cycle at TP = 240°C (X = 0.06 m). [Color figure can be viewed in the online issue, which is available at www.interscience.wiley.com.]

increasing filling time. When the cooling time decreases (higher flow rate of polymer), the solidification layer adjacent to the mold wall decreases as shown in Figure 17. Contrarily, for lower polymer flow rate, a thick layer of solid is formed beside the mold walls where this layer prevents the polymer to reach the edges of the mold cavity. Thus, it leads to form an air trap at these places as shown in Figure 18. These positions of unfilled mold cavity of polymer yield a defect on the final product quality. The results show that increasing the filling time by about 60% increases the solidification percent by about 500%.

Effect of injection temperature

One of the most important process conditions is the temperature of the polymer melt in the injection molding process. Melt temperature is a very important parameter that influences process features such as cycle times, crystallization rates, degree of crystallinity, melt flow properties, and molded product qualities. When the polymer temperature increases, the power consumed to heat the polymer increases. The higher the melt temperature, the larger the shrinkage and warpage of the injection molded part. However, high melt temperature lowers the melt viscosity, and therefore increases the mobility of the polymer. When the polymer viscosity decrease, thus leads to decreasing the viscous resistance hence the required filling pressure decreases. The melt temperature is not only the criterion for plastics to flow, but it also can be the guideline to predict the quality of the molded parts. The effect of the polymer temperature on the time required to completely solidifying the material to be ejected of the mold is shown in Figure 19. Figure 19 shows that an increase in the polymer temperature of about 20% increases the cooling time of about 10%. The value of the injection polymer temperature determines the solidification percentage of the material during the filling stage which affects the percentage of filled volume of the cavity by polymer material as stated. The evolution of the solidification percent of the product at the end of filling stage for different injection temperatures of the plastic material at different injection molding cycles is shown in Figure 20. Figure 20 shows that when the polymer temperature increases the solidification percent at the end of filling stages decreases. It also shows that with increasing injection molding cycles, the solidification percent decreases due to heating of the mold material.

The inlet polymer temperature also affects the final temperature and temperature distribution through the product when it is ejected from the

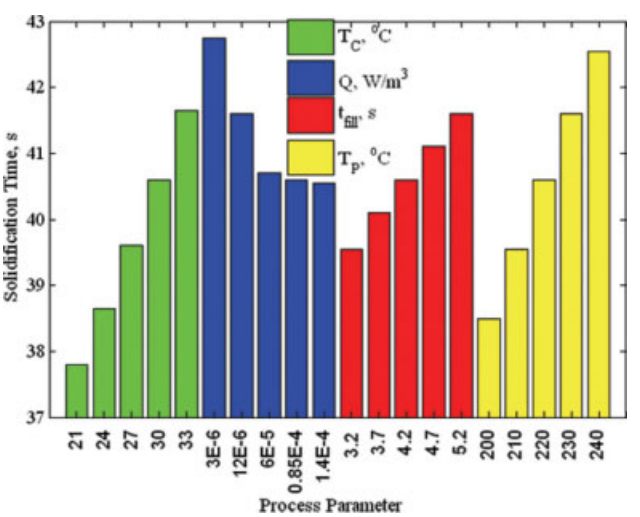

Figure 23 Changing the solidification time with variation of process parameters. [Color figure can be viewed in the online issue, which is available at www.interscience.wiley.com.]

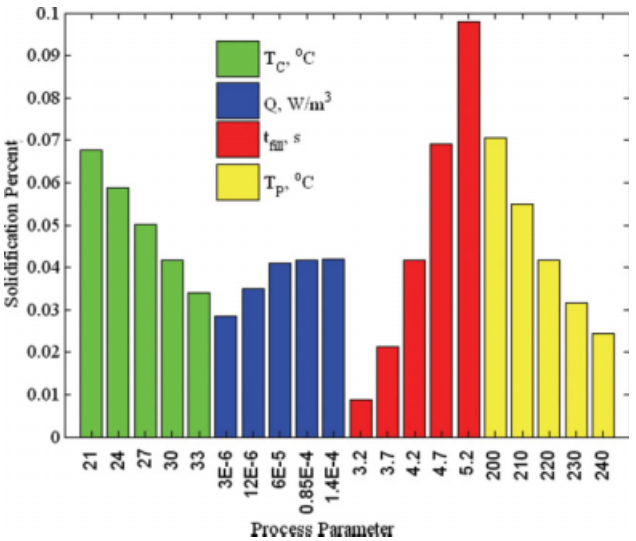

Figure 24 Changing the solidification percent at the end of filling stage with variation of process parameters. [Color figure can be viewed in the online issue, which is available at www.interscience.wiley.com.]

mold cavity. These have a strong relation with final properties of the molded product as indicated. The effect of the injection temperature on the temperature distribution through the product at the end of cooling stage for the section *YZ* at an injection temperature of 200°C and 240°C are shown in Figures 21 and 22, respectively. The results are shown for the 30th injection molding cycle. The figures show that the temperature of the thick part is greater than that of thin part, which requires increasing the cooling of the thick part to arrive a homogenous temperature. They also show that beneath the cooling channel of the thin part, a separation in the temperature distribution occurs, which negatively affects the final product quality. The figures indicate that the maximum temperature of the product at the end of the cooling is greater in case of higher injection temperature (about 95°C in case of an injection temperature of 240°C and 80°C for an injection temperature of 200°C). From the earlier results, it is found that increasing injection temperature increases the cooling time, decreases the solidification percent during the filling stage, and decreases the injection pressure and must economize between those effect to achieve the optimum conditions.

Figures 23–25 show the effect of different process parameters (T_c, Q_c, t_{fill}, and T_P) on the solidification time, solidification percent at the end of filling stage, and maximum difference of temperature of the product at the end of cooling stage, respectively. The results are shown for the 30th injection molding cycle. By comparing the results of the figures, it is found that the coolant temperature and the polymer temperature have great effect on cooling time of the product. Figures 23–25 also show that the solidification of the product during the filling stage is greatly affected by filling time and the temperature of the product at the end of cooling stage is greatly affected by the polymer temperature. From these results, it is found that the process parameters performing the minimum cooling time not necessarily achieves optimum conditions for cavity filling and final temperature of the product. Hence, the selected parameters must be optimized to reach these goals.

CONCLUSION

Three-dimensional study was carried out on the cooling of polymer material by injection molding. The cooling of the injected material was performed by cooling fluid flowing through six cooling channels inside the mold. The effect of process parameters, coolant inlet temperature, coolant flow rate, filling time of polymer material, and its inlet temperature to the mold cavity, were taken during the study. From the results, it is found that the process parameters have a great effect on the injection molding process, the product quality, and the process cost. The results indicate that the time required to completely solidify the product decreases with increasing coolant flow rate and filling time and with decreasing cooling fluid and polymer temperatures. The results indicate that the augmentation of the flow rate of coolant fluid more than 6×10^{-5} m^3/s has a weak effect on the injection molding process. They also show that increasing the filling time leads to incomplete filling of mold cavity. The simulation shows that the operating parameters, which perform

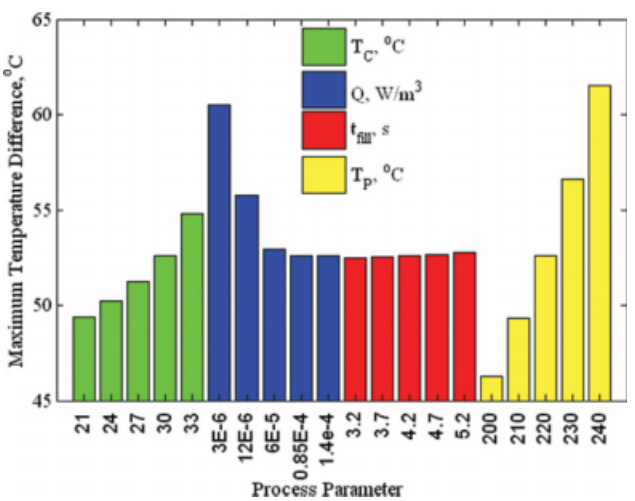

Figure 25 Changing the maximum difference of temperature through the product at the end of cooling stage with variation of process parameters. [Color figure can be viewed in the online issue, which is available at www.interscience.wiley.com.]

minimum cooling time not necessary achieve optimum product quality, and the selected value of the process parameters must be optimized to achieve both goals. The solidification of the product during the filling stage could be minimized and the cooling time could be decreased by heating the mold during the filling stage and cooling the mold during the cooling stage.

NOMENCLATURE

B	polymer material constant, Pa s
C	fractional volume function
C_P	specific heat, J kg^{-1} K^{-1}
f_s	solid fraction
g	acceleration gravity, m s^{-2}
K	permeability, m^2
L	latent heat of fusion, J kg^{-1}
m	mass, kg
N	normal condition
n	power index
p	pressure, Pa
Q	flow rate, m^3 s^{-1}
S_c	source term, W m^{-3}
T	temperature, K
t	time, s
T_b	polymer material constant, K
V	velocity, m s^{-1}

Greek symbols

τ^*	critical stress level, Pa
τ	viscous shear stress tensor, Pa
μ	dynamic viscosity, Pa s
η	shear rate viscosity, Pa s
φ	viscous dissipation term, W m^{-3}
β	polymer material constant, Pa^{-1}
ρ	density, kg m^{-3}
λ	thermal conductivity, W m^{-1} K^{-1}
$\dot{\gamma}$	equivalent shear rate, s^{-1}
η_0	zero shear rate viscosity, Pa s
Γ_1	entry region to the mold cavity
Γ_2	entry region to the cooling channels

Subscripts

a	air
B	sensitivity parameter
c	cooling fluid
f	phase change temperature
fin	final
fill	filling
l	liquid
i	initial
p	polymer
∞	ambient condition
s	solid

References

1. Dimla, D. E.; Camilotto, M.; Miani, F. J Mater Process Technol 2005, 164, 1294.
2. Guo, X.; Isayev, A. I.; Guo, L. Polym Eng Sci 1999, 39, 2096.
3. AC Technology. C-Mold Design Guide; AC Technology: Ithaca, New York, 1995.
4. Tang, S. H.; Kong, Y. M.; Sapuan, S. M. J Mater Process Technol 2006, 171, 259.
5. Min, B. H. J Mater Process Technol 2003, 136, 1.
6. Yu, D.; Wang, X.; Wang, Y. Int Polym Process XXIII 2008, 5, 439.
7. Chen, W.-C.; Fu, G.-L.; Tai, P.-H.; Deng, W.-J. Expert Syst Appl 2009, 36, 1114.
8. Malguarnera, S. C.; Manisali, A. Polym Eng Sci 1981, 21, 586.
9. Bushko, W. C.; Stokes, V. K. Polym Eng Sci 1995, 35, 365.
10. Bushko, W. C.; Stokes, V. K. Polym Eng Sci 1996, 36, 322.
11. Lau, H. C. W.; Ning, A.; Pun, K. F.; Chin, K. S. J Mater Process Technol 2001, 117, 89.
12. Wu, C.-H.; Liang, W. J. Polym Eng Sci 2005, 45, 1021.
13. Chiang, K.-T.; Chang, F. P. Int Commun Heat Mass Transfer 2006, 33, 94.
14. Ghosh, S.; Viana, J. C.; Reis, R. L.; Mano, J. F. Polym Eng Sci 2007, 47, 1141.
15. Chiang, H. H.; Hieber, C. A.; Wang, K. K. Polym Eng Sci 1991, 31, 116.
16. Luisa Alexandra, R. Viscoelastic Compressible Flow and Applications in 3D Injection Moulding Simulation, PhD Thesis, L'école national superior des mines des, Paris, 2004.
17. Vincent., S. Modélisation d'écoulements Incompressibles des Fluides non Miscibles, PhD Thesis, Bordeaux 1 University, France, 1999.
18. Le Bot, C. Impact et Solidification de Gouttes Métalliques sur un Substrat Solide, PhD Thesis, Bordeaux 1 University, France, 2003.
19. Le Bot, C.; Arquis, E. Int J Therm Sci 2009, 48, 412.
20. Arquis, E.; Caltagirone, J. P. C. R. Acad Sci Sér IIb 1984, 299, 1.
21. Vincent, S.; Caltgirone, J. P. J Comput Phys 2000, 163, 172.
22. Angot, Ph. Contribution à l'étude des Transferts Thermiques dans les Systèmes Complexes. Application aux Composants Électroniques, PhD Thesis, Bordeaux 1 University, France, 1989.
23. Khadra, K. Méthodes Adaptatives de raffinement Local Multi Grille, Applications aux Équations de Navier-Stokes et de L'énergie, PhD Thesis, Bordeaux 1 University, France, 1994.
24. Gao, D. M. Int J Numer Methods Fluids 1999, 29, 877.
25. Hassan, H.; Regnier, N.; Lebôt, C.; Defaye, G. Ploymer Eng Sci 2009, 5, 993.
26. Qiao, H. Int Com Heat Mass Transfer 2005, 32, 315.
27. Pavel, S.; Suresh, G. A. Int J Numer Methods Eng 2004, 61, 1501.
28. Igor, J. Catic Polym Eng Sci 1979, 19, 893.
29. Tang, Q. Finite Elem Anal Des 1997, 26, 229.
30. Chen, S.-C.; Li, H. M.; Hwang, S.-S.; Wang, H. H. 2008, 35, 822.
31. Liu, S.-J.; Su, P.-C. Polym Test 2009, 28, 66.
32. Matsumori, T.; Yamazalu, K.; Matsui, Y. Int Fed Inf Process 2006, 199, 161.
33. Pearson, J. R. A. Polym Eng Sci 1978, 18, 222.
34. Howard, W. C.; Mentzer, C. C. Mentzer Polym Eng Sci 1986, 26, 488.